

Promising Thermoelectric Properties of Commercial PEDOT:PSS Materials and Their Bi₂Te₃ Powder Composites

B. Zhang,[†] J. Sun,[†] H. E. Katz,^{*,†} F. Fang,[‡] and R. L. Opila[‡]

Department of Materials Science and Engineering, Johns Hopkins University, 206 Maryland Hall, 3400 North Charles Street, Baltimore, Maryland 21218, United States, and Department of Materials Science and Engineering, University of Delaware, 301 Spencer Laboratory, Newark, Delaware 19716, United States

ABSTRACT Newly commercialized PEDOT:PSS products CLEVIOS PH1000 and FE-T, among the most conducting of polymers, show unexpectedly higher Seebeck coefficients than older CLEVIOS P products that were studied by other groups in the past, leading to promising thermoelectric (TE) power factors around 47 $\mu\text{W}/\text{m K}^2$ and 30 $\mu\text{W}/\text{m K}^2$ respectively. By incorporating both n and p type Bi₂Te₃ ball milled powders into these PEDOT:PSS products, power factor enhancements for both p and n polymer composite materials are achieved. The contact resistance between Bi₂Te₃ and PEDOT is identified as the limiting factor for further TE property improvement. These composites can be used for all-solution-processed TE devices on flexible substrates as a new fabrication option.

KEYWORDS: thermoelectric • composite material • conducting polymer • bismuth telluride • poly(3,4-ethylenedioxythiophene) poly(styrenesulfonate) • interface resistance

INTRODUCTION

The global demand for affordable, renewable, and clean energy resources to reduce our dependence on carbon-based fossil energy leads to important research approaches, including thermoelectric (TE) energy conversion. Abundant solar, geothermal, and automobile-derived heat can be directly converted into clean electricity via TE devices that are solid-state, quiet, compact and maintenance-free (1–3). In a simplified model, the performance of thermoelectric materials is determined by a dimensionless quantity called the Figure of merit, ZT , defined by

$$ZT = S^2\sigma T/\kappa \quad (1)$$

where S is the Seebeck coefficient (thermoelectric power, the change in voltage per unit temperature difference in a material), σ is the electrical conductivity, T is temperature in Kelvin at which the properties were determined, and κ is the thermal conductivity. The state of the art of several currently used TE materials is a ZT value around 1 (4), defining their efficiency of cooling or power generation to be 10–30% of that of conventional thermal engines.

Most ongoing research focuses on inorganic TE materials: semiconductors such as Bi₂Te₃, CoSb₃, SiGe, MgSi; conducting oxides, for example, NaCo₂O₄ and CaMnO₃; and metal alloys, such as BiSb (5, 6). An alternative TE research

approach, organic or polymer thermoelectric materials, has been given relatively less attention, mainly because of the application temperature restriction: few semiconducting polymers are stable at high temperatures in the range of 500–900 K, which is the most favorable temperature range for massive TE energy recovery. Also, the Figure of merit of these materials is low, usually 2–3 orders of magnitude lower than inorganic TE materials. However, TE polymers could be of great interest in some niche applications for room temperature cooling and power generation on the micro scale. For example, because of the extremely high integration of present electronic devices, heat generated by electric current needs to be removed from devices in order to maintain stable performance, and wireless sensors need off-grid and battery-free power supplies to work in remote areas or a portable manner. Other potential applications include providing power for cochlear hearing replacements, nerve stimulation implants, thermal charge LED lights, and light-emitting diode and photodetector coolers (7). In these niche applications, efficiency may not be the most important factor to be considered as long as the electrical power or cooling power is sufficient. Other attributes such as weight, size, and flexibility may be of greater importance, and these are inherent advantages of organic or polymer TE materials compared to inorganic TE materials. Because of the flexible nature of polymers, polymer TEs can be easily integrated into unusual topologies to fit the geometrical requirements of most applications and could also possibly maximize the heat absorbing area, leading to an enhanced practical efficiency compared to rigid inorganic TE devices (8–10). The lightweight of polymers is also favored because of the demand for the portability of these devices. The printability of polymers can reduce the manufacturing cost dramatically

[†] Johns Hopkins University.

[‡] University of Delaware.

Received for review July 26, 2010 and accepted October 15, 2010

DOI: 10.1021/am100654p

2010 American Chemical Society

as well, compared to inorganic thin-film deposition techniques, which are utilized for Bi_2Te_3 microcooling and power-generation devices by TE device-making companies, such as Nextile and Thermo-life (11). Polymer TE materials could have a very promising future in these applications if both n and p type polymers having a stable ZT comparable to the industry standard, Bi_2Te_3 , could be realized.

Modern conducting polymers can have a stable electrical conductivity in air at the same level as the best inorganic TE material, Bi_2Te_3 , $\sim 10^3 \text{ S/cm}$ and a thermal conductivity much less than Bi_2Te_3 . Slack proposed that the best TE material should possess thermal properties similar to that of a glass and electrical properties similar to that of a perfect single crystal material (a phonon glass/electron crystal, PGEC), that is, a poor thermal conductor and a good electrical conductor (12). In this regard, the conducting polymer is essentially a phonon glass electron glass (PGEG) material.

The main challenge so far for polymer TEs is the difficulty of obtaining a large Seebeck coefficient and a large electrical conductivity simultaneously (13, 14). Engineering the electronic structure of polymers to have a favorable density of states and Fermi level is the key to solving the problem. However, there is little or no precedent for Seebeck and electrical conductivity increasing simultaneously with doping for polymer TE materials, other than our recent publication demonstrating a simultaneous increase in Seebeck coefficient and conductivity in a doped poly(alkylthiophene) blend with defined density of states (15).

There have been some reports of TE properties of polymers beginning in the 1990s (14, 16–21). The stable ZT is on the order of $10^{-2} \sim 10^{-3}$, much lower than inorganic materials. Recent works have involved conducting polymers such as polyaniline (PANI) and PEDOT:PSS filled with carbon nanotubes (22, 23) or single-phase, highly conducting polymers (24). In these investigations, the power factors of as-synthesized polymer or polymer composites are ca. $5\text{--}50 \mu\text{W/m K}^2$. The typical electrical conductivity value is from several tens to several hundred S/cm and the Seebeck coefficient of the sample with best power factors is around $20\text{--}30 \mu\text{V/K}$. Because it is technically very challenging to measure in-plane thermal conductivity of thin films at room temperature; some groups use cross-plane thermal conductivity as an estimate, or only report the power factor. A material like PEDOT can have a very anisotropic electrical conductivity (25); so the thermal conductivity of the in-plane direction could also be larger than in the out-of-plane direction if thermal conductivity is correlated with electrical conductivity as in most TE materials.

Poly(3,4-ethylenedioxythiophene) poly(styrenesulfonate) (PEDOT:PSS) is the most commonly used polymer for printed electrodes and other passive elements because of its high conductivity, excellent stability, flexible mechanical properties, and transparency (26). PEDOT itself is insoluble in most common solvents. However, PEDOT emulsified by PSS can be well dispersed in aqueous solvent. In the mixture of PEDOT and PSS, PEDOT is responsible for conducting charges and PSS is insulating. Because of the coexistence of

conducting PEDOT and insulating PSS, the electrical conductivity is strongly dependent on the morphology and microstructure of the film. The presently proposed model of the microstructure of conducting PEDOT:PSS thin film is that the dry film of the PEDOT:PSS is made by grains of PEDOT-rich cores with a diameter of $30\text{--}40 \text{ nm}$ and PSS shells with a thickness about $5\text{--}10 \text{ nm}$. Carriers hop from one grain to another to conduct the electrical current. This model has been supported by spectroscopic and microscopic evidence including X-ray and ultraviolet photoelectron spectroscopy (XPS and UPS), X-ray diffraction, and tunneling microscopies (STM, HAADF-STEM). The hydrogen bonding by HSO_3 groups of PSS-rich shells provides the adhesive force between grains. The flexibility of the PEDOT:PSS film is because of this adhesive force (27, 28).

The TE properties of PEDOT have been studied by several groups. This research was based on Bayton P and Bayton PH510 products that were reported to have electrical conductivities and Seebeck coefficients of 50 S/cm and $13 \mu\text{V/K}$; and 300 S/cm and $13 \mu\text{V/K}$, respectively, with 5% DMSO doping (29, 30). It was clearly shown that from Bayton P to Bayton PH510 the electrical conductivity can increase while the Seebeck coefficient can be kept at the same level, demonstrating a potential improvement for the TE properties of PEDOT:PSS. By adding a significant amount of carbon nanotubes into PEDOT, Yu et al. reported samples having up to 400 S/cm electrical conductivity and around $25 \mu\text{V/K}$ Seebeck coefficient, contributing to a high power factor for polymers of $25 \mu\text{W/m K}^2$ (22).

Recently, H.C.Stark, Inc., began offering another two conductive polymer products, CLEVIOS PH1000 and CLEVIOS FE-T. CLEVIOS PH1000 is an aqueous dispersion of PEDOT/PSS having the best electrical conductivity among CLEVIOS products, almost the same as commercialized TE ingot Bi_2Te_3 . CLEVIOS FE-T is made as a formulation containing binder resins and functional additives designed for better film quality and processability. In the work we report here, we have found that the two new products not only have good electrical conductivity but also a relatively large Seebeck coefficient. The combination results in these commercialized PEDOT:PSS having a power factor value among the highest reported levels for polymer TE materials. This discovery alters two common but incorrect impressions about PEDOT:PSS as a TE material: (1) the Seebeck coefficient of PEDOT is no larger than $12\text{--}13 \mu\text{V/K}$ if the composition is essentially the same; (2) the increase of the electrical conductivity of PEDOT:PSS will lead to the decrease of Seebeck coefficient, as would be the case for most conducting polymers. The mechanism behind this could have a dramatic effect on polymer TE research.

To further improve the TE performance of the PEDOT:PSS, we also utilized the known high performance of commercialized Bi_2Te_3 , mixing it as a powder with PEDOT:PSS, realizing a 2–3 fold increase for the power factor. These experiments demonstrate a promising route of making TE slurry materials which can be used for printing TE devices on flexible substrates.

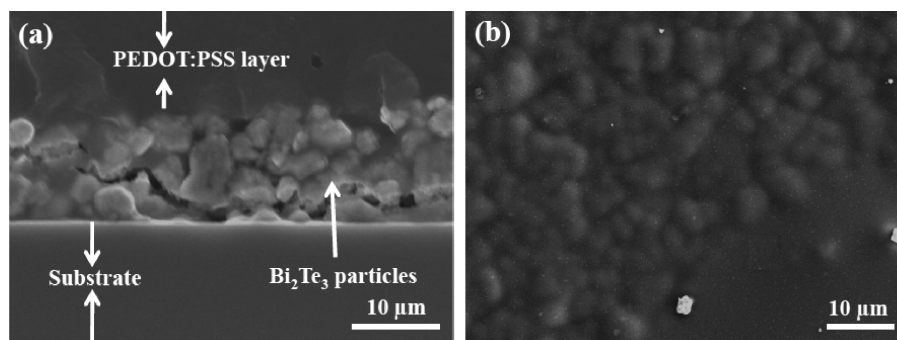


FIGURE 1. (a) Cross section SEM picture of the PH1000 mixed with Bi₂Te₃ ball milled particles (30% volume ratio of PEDOT:PSS). (b) Top view of the sample.

EXPERIMENTAL SECTION

CLEVIOS P, CLEVIOS FE-T, CLEVIOS PH500, and CLEVIOS PH1000 were purchased from H.C.Stark. Dropcasting was used to make films several μm thick on prepatterned gold electrodes that had been deposited on the glass slide in a vacuum evaporator. The drop cast samples were first kept on a hot plate at 50 $^{\circ}\text{C}$ for 1 h to remove liquid slowly. We found that if the liquid were vaporized too fast, the film surface is very rough. Then, the hot plate was heated to 120 $^{\circ}\text{C}$ and kept at 120 $^{\circ}\text{C}$ for 15 min to completely remove all of the liquid. Typical samples are 4 mm wide, 7.5 mm long, and 3–10 μm thick. Since the density of solid content of these products is known, the film thickness could be estimated by using the volume of the sample divided by the product of the width and length of the samples. Profilometry was utilized to confirm the accuracy of our estimation.

Conductance was measured by obtaining I – V curves on a semiconductor parameter analyzer. The Seebeck coefficient (S) was measured by mounting a sample on a thermoelectric heater-cooler pair, with one electrode of the sample over each. Thermal EMF (ΔV) and temperature difference (ΔT) were measured simultaneously by probing the pair of electrodes with a source meter and thermometer and feeding the data into a computer. Numerous measurements of ΔV , typically 50, were made for each value of ΔT , with a standard deviation of 1–5% (0.01–0.05 mV) per data set. These ΔV were averaged to eliminate the noise signal induced by the environment. Several temperature differences (ΔT) were imposed on the sample. The slopes of plots of ΔV versus ΔT gave values of S . The linearity of the data of ΔV and ΔT was used as a key criterion to ensure valid measurements. The coefficient of determination, r^2 , was invariably above 0.99. Copper wire was used for voltage leads and has very small Seebeck coefficient (1.94 $\mu\text{V}/\text{K}$) as compared to our samples; therefore, the thermoelectric effect from the voltage leads could be neglected. The Seebeck coefficient measurement was also calibrated by a pure Ni metal sample that is widely utilized as a standard sample for calibrating Seebeck measurement (31, 32). A very good agreement between our result ($-21.4 \pm 0.4 \mu\text{V}/\text{K}$) and reported values (-19.5 and $-20.5 \mu\text{V}/\text{K}$) demonstrates the accuracy of our Seebeck coefficient data.

Bi₂Te₃ powders were made by pulverizing a p-type BiTe ingot, purchased from Marlow industries, Inc. The ball mill system is spex 8000. The whole ball mill process was carried out for 30 min in inert atmosphere to avoid oxidizing the particle surfaces. The ball milled powder needs to be rinsed in 5 wt % HCl to remove the oxidized layers on the surface before mixing with PEDOT:PSS. This process is very important. Without HCl rinsing, the power factor of the composite material is much smaller than the ones obtained with HCl rinsing. After rinsing with 5% HCl in water, 3–4 mg Bi₂Te₃ ball milled particles were dispersed in alcohol and drop-cast on a 7.5 mm \times 4 mm area on a glass slide with prepatterned gold electrodes. After the alcohol vaporized, a thin layer of Bi₂Te₃ particles formed on the substrate.

Different amounts of PEDOT:PSS solution were drop-cast on the top of the a thin layer of Bi₂Te₃ particles. The first PEDOT:PSS solution entered the spaces among the particles, and then with the addition of more PEDOT:PSS, a continuous layer of PEDOT:PSS formed on the top of the particles. The resulting film is very rough. Therefore, the thickness was estimated by using the volume of the PEDOT:PSS and Bi₂Te₃ divided by the sample area. The sample thickness varies from 10 to 20 μm depending on different amounts of the PEDOT:PSS. We also tried to stir Bi₂Te₃ powders in the PEDOT:PSS solution; however, the resulting films are very easily delaminated during the drying process. It is possible that the stirring process destroys the emulsion structure of PEDOT:PSS in aqueous liquid because of the large hydrophilic surface area of the Bi₂Te₃ particles. Two representative SEM pictures are shown in Figure 1. On the cross section picture taken from the fracture surface, we can see that PEDOT:PSS exists among the Bi₂Te₃ micrometer size particles and also a thin layer of PEDOT:PSS is formed on the top. From the top view picture, the rough surface of samples is revealed. These Bi₂Te₃ particles are not uniformly dispersed in the PEDOT:PSS film.

The X-ray photoemission spectroscopy (XPS) analysis performed on the Bi₂Te₃ surface is consistent with our hypothesis that the HCl can remove the oxide layer from Bi₂Te₃ surface. Using the PHI 5600 XPS System, the spectra were acquired with incident radiation from an monochromatic Al–K α X-ray source at 1486.6 eV, and a spherical energy analyzer. XPS spectra were taken on a thin slide of Bi₂Te₃ material sample which is cut from a Bi₂Te₃ ingot and polished down to less than 1 mm thick with a mirror-like surface. One wt % HCl acid was used to etch the XPS Bi₂Te₃ sample instead of 5 wt % HCl because we consider that there is less oxidized surface on the Bi₂Te₃ slide used for XPS than the powder used for making composites.

RESULTS AND DISCUSSION

CLEVIOS P, CLEVIOS PH500, and CLEVIOS PH1000 products are all aqueous dispersions of the intrinsically conductive polymer PEDT/PSS [poly(3,4-ethylenedioxythiophene)/poly(styrene sulfonate)]. CLEVIOS PH1000 is tailored to a high conductivity and forms conductive coatings showing the best electrical conductivity, > 900 S/cm, among all CLEVIOS products. CLEVIOS P and CLEVIOS PH500 are older version products with less conductivity. The exact mechanism enhancing the electrical conductivity of PH1000 products is unknown.

Figure 2 shows the electrical conductivity, Seebeck coefficient and power factor for the three P series products including effects of different dimethyl sulfoxide (DMSO) additive concentrations and one CLEVIOS FE-T which had already been formulated and did not contain DMSO. Al-

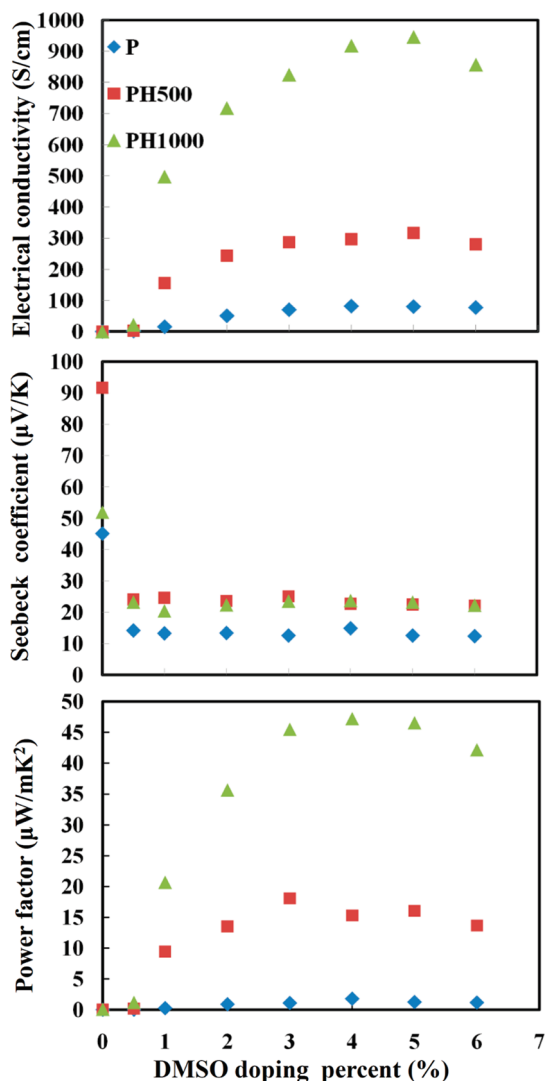


FIGURE 2. Electrical conductivity, Seebeck coefficient and power factor of CLEVIOS P, PH500 PH1000.

though the value of electrical conductivity and Seebeck coefficient is different for the three P series products, the trend in terms of DMSO addition is almost identical. The electrical conductivity of all three PEDOT grades increases significantly when the DMSO level approaches 1 %, shows a monotonically continuous increase up to 5 % DMSO, then starts to decrease. These results were consistent with electrical property information provided by H.C. Stark, Inc. We found that the Seebeck coefficient started a steep fall when the DMSO level exceeded 0.5 %. There is no obvious correlation between DMSO amount and Seebeck coefficient when the DMSO content is more than 1 %. Kemerink et al propose that the addition of high-boiling solvents like sorbitol and DMSO to the aqueous dispersion used for film deposition rearranges PEDOT-rich clusters into elongated domains. This model has been supported by STM and AFM (27). If this model is correct, a plausible explanation is that when the DMSO level is more than 1 %, the DMSO only increased the number of connected elongated PEDOT:PSS grains but did not change any carrier scattering mechanism and the energy barrier which needs to be overcome for a carrier moving

Table 1. Thermoelectric Properties of Different Clevios PEDOT Products

	electrical conductivity (S/cm)	Seebeck coefficient ($\mu\text{V/K}$)	power factor ($\mu\text{W/mK}^2$)
Clevios p (5% DMSO)	81.9	12.6	1.28
Clevios PH500 (5% DMSO)	317	22.5	16.05
Clevios PH1000 (5% DMSO)	945	22.2	46.57
Clevios FET	320	30.3	29.39

from one grain to another, because if any of the three had changed, a change in Seebeck coefficient should have been observed.

PH1000 products showed a power factor superior to other products at all DMSO levels more than 1 %. The best power factors, $47 \mu\text{W/m K}^2$, are from 4 % and 5 % DMSO in CLEVIOS PH1000. This power factor is among the highest power factors for pure organic materials. It is a significant discovery that in the PEDOT:PSS system, both electrical conductivity and thermopower can be improved from P to PH1000, which are claimed to have very similar chemical composition.

The mechanism behind this has considerable scientific importance. For most semiconductor polymers, increasing the electrical conductivity will detrimentally affect the Seebeck coefficient, usually leading to a small power factor. There are different models pertaining to the mechanisms of improving the electrical conductivity of PEDOT:PSS. None of them take into account the possibility of increasing Seebeck coefficient as well. Our previous work (15) demonstrates a route for designing thermoelectric materials by which the increases in Seebeck coefficient and conductivity do not cancel each other. The core idea of the design is to blend two semiconductor polymers with similar but non-identical Fermi levels. This situation is effectively equivalent to having a large derivative of density of states with respect to the Fermi level. It would be interesting to uncover whether an analogous mechanism applies to the PEDOT formulations.

In another case, CLEVIOS FE-T is made as a formulation containing binder resins and functional additives. On the basis of the listed composition, the CLEVIOS FE-T contains 1,2-ethanediol and 1,4-dioxane instead of the water included in CLEVIOS P series products. Films derived from CLEVIOS FE-T will wet and adhere better to different substrates than P series products, have improved mechanical strength, and resist environmental degradation. CLEVIOS FE-T product containing nonconductive binders showed an increased Seebeck coefficient, $30.3 \mu\text{V/K}$, which is one of highest Seebeck coefficient for pure or composite PEDOT:PSS films, demonstrating that these nonconductive binders can also play a role in improving the Seebeck coefficient. The electrical conductivity and Seebeck coefficient data of FE-T are also shown in Table 1 along with other Clevios products. As for the TE application, at the same power factor level, CLEVIOS FE-T is more favorable because of its good film quality and processability.

There are few reports about the thermal conductivity of PEDOT:PSS films. The only report known to us is from Jiang

et al. reporting a thermal conductivity 0.17W/m K for the Bayton P product which is doped with 10 % DMSO and has 30S/cm electrical conductivity.

The Wiedemann–Franz–Lorentz relation derived from classical Drude theory defines the relationship between electrical conductivity and thermal conductivity, and has been widely used to estimate phonon thermal conductivity (K_p) and carrier thermal conductivity (K_e) for Fermion liquid systems such as metals or degenerate semiconductors.

$$K = K_p + K_e \quad (2)$$

(K is total thermal conductivity)

$$K_e = L\sigma T \quad (3)$$

(L is Lorenz number, theoretically $2.44 \times 10^{-8} \text{ W } \Omega \text{ K}^{-2}$; σ is electrical conductivity; T is the temperature). The experimental value for L ranges from $L = 2.23 \times 10^{-8} \text{ W } \Omega \text{ K}^{-2}$ for copper at 0 °C to $L = 3.2 \times 10^{-8} \text{ W } \Omega \text{ K}^{-2}$ for tungsten at 100 °C. Chester and Thellung demonstrated that the L is exactly $\pi^2/3(K_B/e)^2$ for a noninteracting electron system with arbitrary scattering strength (33). Castellani et al. argued that even in electron interacting systems, the L value is still close to the theoretical value (34). Therefore, a universal Lorenz number could be considered to be one of the defining characteristics of Fermion liquid (35). A conducting polymer naturally has a 1-D electron transport characteristic, possibly showing a non-Fermi liquid behavior. Kane et al. (35) argued that conducting polymers could be quasi-1-D electron systems, displaying characteristics of a Luttinger liquid phase in which the Lorentz number is modified. For PEDOT:PSS system (CLEVIOS PVP), Nardes et al showed that DMSO doping caused electron transport to change from 3D variable range hopping (VRH) to 1D VRH (28). The theoretical calculation of Casian et al. showed that in some highly conducting quasi-one-dimensional organic crystals the Wiedemann–Lorentz–Franz law is strongly violated and the Lorentz number could be reduced more than ten times as crystals become imperfect, favoring the TE properties significantly (36). Further work to determine the thermal conductivity of our PEDOT samples could help reveal the thermal transport mechanism of this polymer.

Figure 3 shows the TE properties of the mixture of CLEVIOS PH1000 and n/p-type Bi_2Te_3 ball-milled powders. Bi_2Te_3 powders have a non uniform size distribution from submicrometer to several micrometers. The power factor of the mixture using PH1000 is generally better than other products due to the best power factor associated with PH1000. The three highest power factors, 131, 113, and 119 $\mu\text{W}/\text{m K}^2$, are respectively from the samples with 10 vol %, 17 vol % and 23 vol % of PEDOT. The general trend is that the electrical conductivity increased and Seebeck coefficient decreased with increase of PEDOT volume ratio. If we use the Wiedemann–Franz–Lorentz relationship to estimate the carrier thermal conductivity, the carrier thermal conductivity of the samples having 10 %, 17 %, and 23 % of PEDOT are

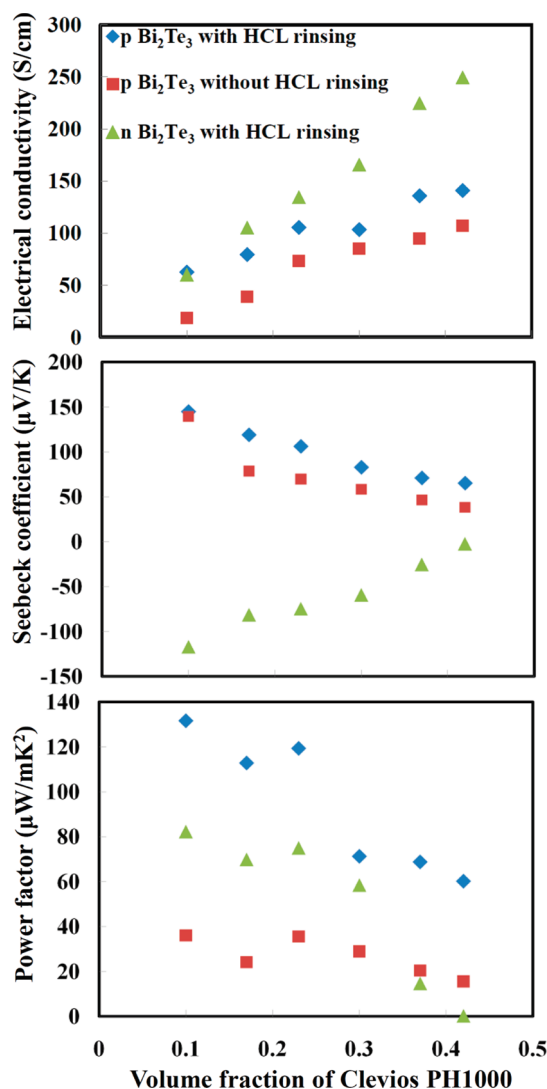


FIGURE 3. Electrical conductivity, Seebeck coefficient, and power factor of CLEVIOS PH1000 mixed with Bi_2Te_3 particles

0.043, 0.055, and 0.073 W/m K, respectively. The lattice thermal conductivity can be estimated by considering the lattice thermal conductivity of PEDOT:PSS and Bi_2Te_3 in a parallel model that gives an upper limit for a two-phase system. The lattice thermal conductivity of Bi_2Te_3 is estimated by using total thermal conductivity 1.28 W/m K, which is from the technical information provided by Marlow Inc. subtracting the carrier thermal conductivity 0.73W/m K obtained from Wiedemann–Franz–Lorentz relationship. The upper limit of lattice thermal conductivity of the three samples 10 %, 17 %, and 23 %, are $0.55 \times 0.90 + 0.2 \times 0.10 = 0.515\text{W}/\text{m K}$, $0.55 \times 0.83 + 0.2 \times 0.17 = 0.498\text{W}/\text{m K}$, $0.55 \times 0.77 + 0.2 \times 0.23 = 0.470\text{W}/\text{m K}$ respectively. The estimated total thermal conductivity equals 0.558 W/m K, 0.553 W/m K and 0.543 W/m K for 10 %, 17 % and 23 % samples respectively. The real thermal conductivity of these samples could be less than these values because the interface phonon scattering between two materials is not considered here. The estimated ZT for the three samples should be more than 0.08 (10 %), 0.06(17 %), and 0.07(23 %). The

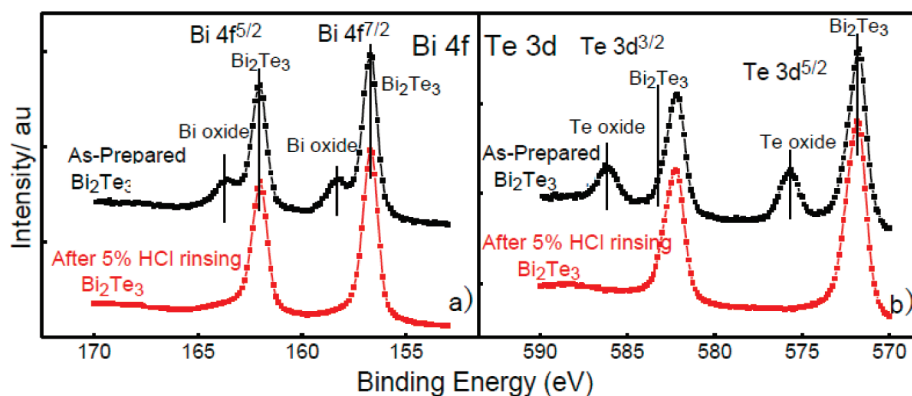


FIGURE 4. XPS spectra of core levels of Bi_2Te_3 surface: (a) Bi 4f of Bi_2Te_3 and Bi oxides and (b) Te 3d of Bi_2Te_3 and Te oxides.

PEDOT content has to be more than 20 vol % in order to wet and adhere all the powders well and show some flexibility.

Even though during the ball milling and storage, all possible means in our lab are used to avoid the formation of an oxidation layer on the Bi_2Te_3 surface, there are still oxidized layers forming on the Bi_2Te_3 particles, confirmed by X-ray photon spectroscopy (XPS). The XPS spectra taken on Bi_2Te_3 surfaces before and after HCl rinsing are shown in Figure 4. Clearly the characteristic peaks of Bi–O and Te–O chemical states are completely removed after HCl rinsing and the peaks associated with Bi_2Te_3 remain at the same position. These results are of great importance not only for the research herein but also for the other thermoelectric nanocomposites research because numerous semiconductor or metal alloy nanostructures of thermoelectric materials face the issue of oxidized surfaces in air. In most cases, the oxidation layer is detrimental to thermoelectric properties. In the paper of Poudel et al. (37), it was also claimed that the prevention of oxidation of ball-milled Bi_2Te_3 nanoparticles by doing the experiments in glovebox under Argon atmosphere is especially important to obtain enhanced thermoelectric properties for Bi_2Te_3 nanocomposites made by hotpressing the ball-milled Bi_2Te_3 nanoparticles. We think that simply using acid to remove the oxidation layer could achieve the same results but in a much more cost-effective way. Further experiments are under way. Removing the oxide can help improve the power factor, which is defined as $S^2\sigma$, the square of Seebeck coefficient multiplied by the electrical conductivity, of these composite materials. In the case where no HCl solution treatment was used to remove the oxides on the surface, both the Seebeck coefficient and electrical conductivity were reduced, leading to a 4–5 fold decrease of power factor, as shown in Figure 3. Similar results were also obtained in the samples using CLEVIOS P, as seen in Figure 5; although the power factor of the composite materials made by CLEVIOS P is lower than samples made from CLEVIOS PH1000. After HCl solution rinsing, both the electrical conductivity and Seebeck coefficient of the composite samples increased. These data demonstrate the dominating importance of the interface in organic/inorganic TE composite materials. The interface can be considered as a third phase in the composite. If a more electrically conducting interface between Bi_2Te_3 and PEDOT

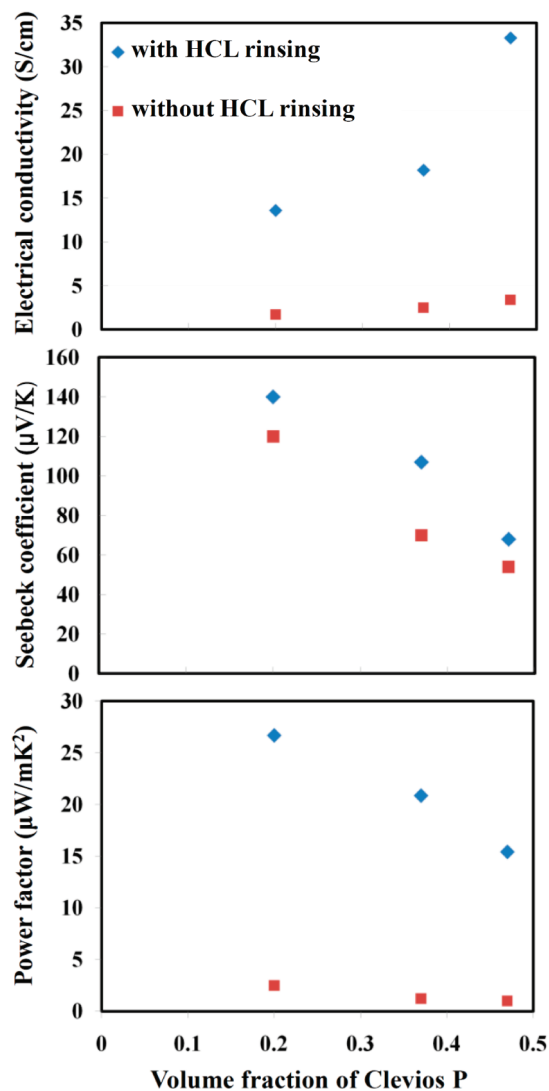


FIGURE 5. Electrical conductivity, Seebeck coefficient, and power factor of CLEVIOS P mixed with Bi_2Te_3 particles.

can be achieved, a further enhancement of the power factor can be expected.

In a binary thermoelectric composite system, we can define the boundaries of electrical conductivity, Seebeck coefficient, thermal conductivity and ZT by using parallel and series modes if the interface is assumed to be neglected. These models are very rough; but it gives us a basic guideline

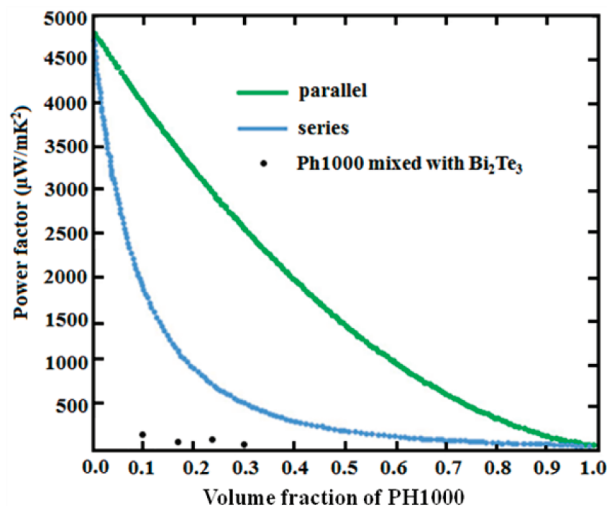


FIGURE 6. Power factor bounds of PH1000 mixed with p-type Bi_2Te_3 powders in parallel and series models.

for designing inorganic and organic TE composite materials. Defining Material A having S_1 , σ_1 , κ_1 , and material B having S_2 , σ_2 , κ_2 (S , σ , κ are denoted for Seebeck coefficient, electrical conductivity, and thermal conductivity), in a series model:

$$S = \frac{S_1 \cdot \left(\frac{1}{\kappa_1}\right) \cdot x}{\frac{1}{\kappa_1} \cdot x + \frac{1}{\kappa_2} \cdot (1-x)} + \frac{S_2 \cdot \left(\frac{1}{\kappa_2}\right) \cdot (1-x)}{\frac{1}{\kappa_1} \cdot x + \frac{1}{\kappa_2} \cdot (1-x)} \quad (4)$$

$$\sigma = \frac{\sigma_1 \sigma_2}{x \sigma_2 + (1-x) \sigma_1} \quad (5)$$

where x is the volume ratio for material A. In a parallel model:

$$S = \frac{S_1 \cdot \sigma_1 \cdot x + S_2 \cdot \sigma_2 \cdot (1-x)}{\sigma_1 \cdot x + \sigma_2 \cdot (1-x)} \quad (6)$$

$$\sigma = \sigma_1 x + \sigma_2 (1-x) \quad (7)$$

The upper and lower bounds of the power factor of the mixture of PH1000 are given by the two models, shown in the Figure 6. The Seebeck coefficient and electrical conductivity for Bi_2Te_3 and Ph1000 are $220 \mu\text{V/K}$, 1000S/cm , and $22 \mu\text{V/K}$, 945S/cm , respectively. The power factor of the samples made by embedding Bi_2Te_3 particles in the PEDOT matrix should be within the boundary, neglecting the interface resistance, because the sample is a mixture of series and parallel connections of the two constituents. However, the power factor of our samples was much lower than the lower bound determined by the series model. The main reason for the lower power factor was the low electrical

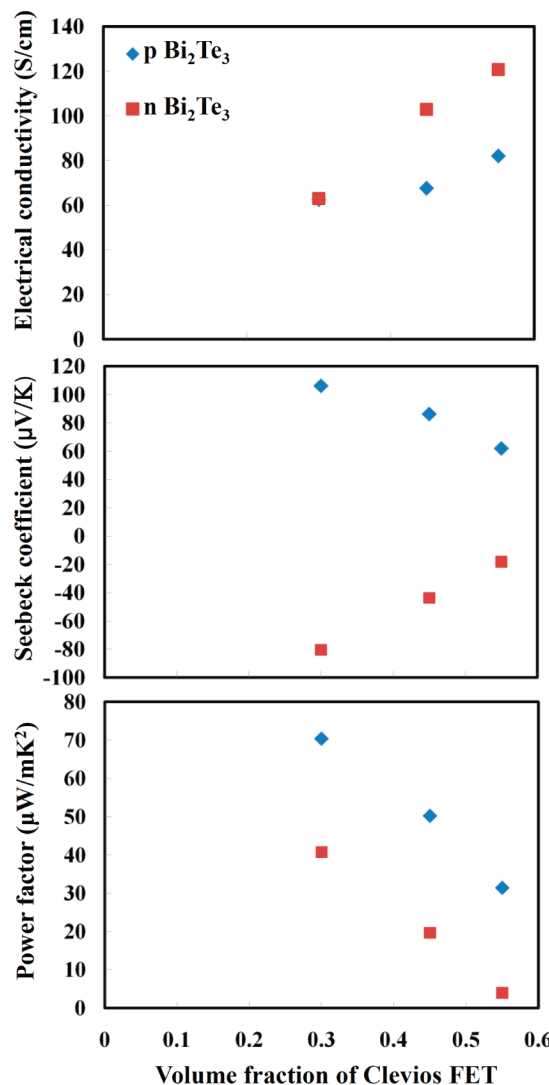


FIGURE 7. Electrical conductivity, Seebeck coefficient and power factor of CLEVIOS FE-T mixed with Bi_2Te_3 particles.

conductivity. Data in Figure 3 show that these composite samples have electrical conductivity around 100S/cm , 1 order of magnitude lower than both PEDOT:PSS and Bi_2Te_3 . The contact resistance from interfaces between PEDOT:PSS and Bi_2Te_3 is identified as the reason for the low conductivity. The contact resistance between Bi_2Te_3 and CLEVIOS P is measured to be $0.004 \Omega\text{cm}^2$ and the one between Bi_2Te_3 and CLEVIOS PH1000 is $0.0025 \Omega\text{cm}^2$. A slightly decrease of contact resistance from CLEVIOS P product to CLEVIOS PH1000 is found. For TE devices, the contact resistance between electrode and TE element has to be $10^{-6} \sim 10^{-7} \Omega\text{cm}^2$, so that the device ZT will not be much less than material ZT. From this, we learn that we need to reduce the contact resistance between Bi_2Te_3 and PEDOT by 3 orders of magnitude to have power factors close to those predicted by the models.

Suggested both experimentally and theoretically, the nanostructured Bi_2Te_3 could have much higher ZT than the bulk counterpart. If Bi_2Te_3 nanostructures can be incorporated into the polymer matrix and interface resistance between the nanostructure and polymer can be reduced to

a level where the superior thermoelectric properties of the nanostructures can be utilized in the composite material, ZT could be further improved.

To make a complete TE module, n-type TE material is necessary. However, it is very difficult to make n-type organic TE materials. Currently the best n-channel polymers have a electrical conductivity around 10 S/cm (38) and may be very unstable in air due to the oxidizing nature of the environment. Here we found that if the p-type PEDOT is mixed with n-type Bi₂Te₃, the Seebeck demonstrates n-type material behavior shown in Figure 3. At the same electrical conductivity level, the Seebeck coefficient value of n-type Bi₂Te₃ mixed with PEDOT is less than the p-type Bi₂Te₃ mixed with PEDOT because some portion of the Seebeck coefficient from n-type Bi₂Te₃ was canceled by p-type PEDOT. When the PEDOT volume ratio reached 42 %, the Seebeck coefficient of n-type Bi₂Te₃ mixed with PEDOT is reduced close to zero. However, this experiment demonstrated a possible route to obtain n-type TE polymer composite materials by loading high conductivity and high Seebeck coefficient n-type powders into a low Seebeck coefficient p-type conducting polymer. These n-type samples with PEDOT volume percent from 10% to 30% have a power factor from 80 to 60 $\mu\text{W}/\text{m K}^2$. Experiments using known n-type polymer matrices, which would add to rather than partially cancel Bi₂Te₃ Seebeck coefficient, are under way.

CLEVIOS FE-T, which has greater mechanical flexibility, is another possible matrix for mixing with inorganic particles. The Seebeck coefficient and electrical conductivity of the sample made by CLEVIOS FE-T and n-type/p-type Bi₂Te₃ are shown in Figure 7. These composite materials exhibited both n and p thermoelectric material behavior when loaded with n- and p-type Bi₂Te₃ powders, respectively. The power factor for p-type composite is from 70 $\mu\text{W}/\text{m K}^2$ to 30 $\mu\text{W}/\text{m K}^2$ when the PEDOT volume ratio changed from 30–55 %. The power factor of n-type composite materials is less than p-type material, ranging from 40 to 5 $\mu\text{W}/\text{m K}^2$. The power factors of the n and p samples using PH1000 and FET at the same PEDOT volume ratios in the range of 30–45 % are very similar.

CONCLUSION

CLEVIOS PH1000 and FE-T demonstrated very promising thermoelectric power factors, among the highest power factors for organic materials without any modification. CLEVIOS products are also promising candidates to be used for organic and inorganic composite materials. Our composite samples showed outstanding power factors for both p and n behaviors. The inorganic constituents are not limited to Bi₂Te₃; many other TE inorganic micro or nano structures such as Si, SiGe, PbTe, and BiSb nanostructures, are of great interest for TE organic/inorganic composite materials. With further improvement of TE polymer and polymer composite material, all-solution processed TE modules could be realized in the future.

Note Added in Proof. During the processing of this manuscript for publication, we became aware of a recent published paper which is highly recommended as a reference about polymer/inorganic thermoelectric composite materials (39).

Acknowledgment. Acknowledgment is made to the donors of the Petroleum Research Fund, Grant Number 47578-AC10, administered by the American Chemical Society, for support of this work.

REFERENCES AND NOTES

- (1) Tritt, T. M.; Subramanian, M. A. *MRS Bull.* **2006**, *31*, 188–194.
- (2) Snyder, G. J.; Toberer, E. S. *Nat. Mater.* **2008**, *7*, 105–114.
- (3) Venkatasubramanian, R.; Siivola, E.; Colpitts, T.; O'Quinn, B. *Nature* **2001**, *413*, 597–602.
- (4) DiSalvo, F. J. *Science* **1999**, *285*, 703–706.
- (5) Chen, G.; Dresselhaus, M. S.; Dresselhaus, G.; Fleurial, J. P.; Caillat, T. *Int. Mater. Rev.* **2003**, *48*, 45–66.
- (6) Tritt, T. M.; Boettner, H.; Chen, L. *MRS Bull.* **2008**, *33*, 366–368.
- (7) <http://www.poweredbythermolife.com/whitepaper.htm>2003.
- (8) Qu, W. M.; Plotner, M.; Fischer, W. J. *J. Micromech. Microeng.* **2001**, *11*, 146–152.
- (9) Glatz, W.; Muntwyler, S.; Hierold, C. *Sens. Actuators, A* **2006**, *132*, 337–345.
- (10) Glatz, W.; Schwyter, E.; Durrer, L.; Hierold, C. *J. Microelectromech. Syst.* **2009**, *18*, 763–772.
- (11) Chen, A.; Koplow, M.; Madan, D.; Wright, P. K.; Evans, J. W. In *IMECE 2009: Proceedings of the Asme International Mechanical Engineering Congress and Exposition, Vol 12, Pts A and B*; American Society of Mechanical Engineers: New York, 2009; pp 343–352.
- (12) Slack, G. In *CRC Handbook of Thermoelectrics*; Rowe, D. M., Ed; CRC Press: Boca Raton, FL, 1995; p 407.
- (13) Gao, X.; Uehara, K.; Klug, D. D.; Tse, J. S. *Comput. Mater. Sci.* **2006**, *36*, 49–53.
- (14) Mateeva, N.; Niculescu, H.; Schlenoff, J.; Testardi, L. R. *J. Appl. Phys.* **1998**, *83*, 3111–3117.
- (15) Sun, J.; Yeh, M. L.; Jung, B. J.; Zhang, B.; Feser, J.; Majumdar, A.; Katz, H. E. *Macromolecules* **2010**, *43*, 2897–2903.
- (16) Yoshino, H.; Papavassiliou, G. C.; Murata, K. *Synth. Met.* **2009**, *159*, 2387–2389.
- (17) Feng, J.; Ellis, T. W. *Synth. Met.* **2003**, *135*, 155–156.
- (18) Pfeiffer, M.; Beyer, A.; Fritz, T.; Leo, K. *Appl. Phys. Lett.* **1998**, *73*, 3202–3204.
- (19) Yan, H.; Ishida, T.; Toshima, N. In *Twentieth International Conference on Thermoelectrics, Proceedings*; IEEE: New York, 2001; pp 310–313.
- (20) Yan, H.; Sada, N.; Toshima, N. *J. Therm. Anal. Calorim.* **2002**, *69*, 881–887.
- (21) Toshima, N.; Yan, H.; Kajita, M. *XXI Int. Conf. Thermoelectr., Proc. ICT '02* **2002**, 147–150.
- (22) Kim, D.; Kim, Y.; Choi, K.; Grunlan, J. C.; Yu, C. H. *ACS Nano* **2009**, *4*, 513–525.
- (23) Meng, C. Z.; Liu, C. H.; Fan, S. S. *Adv. Mater.* **2010**, *22*, 535.
- (24) Aich, R. B.; Blouin, N.; Bouchard, A.; Leclerc, M. *Chem. Mater.* **2009**, *21*, 751–757.
- (25) Nardes, A. M.; Kemerink, M.; Janssen, R. A. J.; Bastiaansen, J. A. M.; Kiggen, N. M. M.; Langeveld, B. M. W.; van Breemen, A.; de Kok, M. M. *Adv. Mater.* **2007**, *19*, 1196.
- (26) Wang, Y. J. *J. Phys.* **2009**, *152*, 012023.
- (27) Nardes, A. M.; Janssen, R. A. J.; Kemerink, M. *Adv. Funct. Mater.* **2008**, *18*, 865–871.
- (28) Lang, U.; Muller, E.; Naujoks, N.; Dual, J. *Adv. Funct. Mater.* **2009**, *19*, 1215–1220.
- (29) Jiang, F. X.; Xu, J. K.; Lu, B. Y.; Xie, Y.; Huang, R. J.; Li, L. F. *Chin. Phys. Lett.* **2008**, *25*, 2202–2205.
- (30) Chang, K. C.; Jeng, M. S.; Yang, C. C.; Chou, Y. W.; Wu, S. K.; Thomas, M. A.; Peng, Y. C. *J. Electron. Mater.* **2009**, *38*, 1182–1188.
- (31) Burkov, A. T.; Heinrich, A.; Konstantinov, P. P.; Nakama, T.; Yagasaki, K. *Measure. Sci. Technol.* **2001**, *12*, 264–272.

- (32) Ponnambalam, V.; Lindsey, S.; Hickman, N. S.; Tritt, T. M. *Rev. Sci. Instrum.* **2006**, *77*, 5.
- (33) Chester, G. V.; Thellung, A. *Proc. Phys. Soc. London* **1961**, *77*, 1005.
- (34) Castellani, C.; Dicastro, C.; Strinati, G. *Europhys. Lett.* **1987**, *4*, 91–96.
- (35) Kane, C. L.; Fisher, M. P. A. *Phys. Rev. Lett.* **1996**, *76*, 3192–3195.
- (36) Casian, A. *Phys. Rev. B* **2010**, *81*, 5.
- (37) Bed Poudel, Q. H.; Ma, Y.; Lan, Y.; Minnich, A.; Yu, B.; Yan, X.; Wang, D.; Muto, A.; Vashaee, D.; Chen, X.; Liu, J.; Dresselhaus, M. S.; Chen, G.; Ren, Z. *Science* **2008**, *320*, 4.
- (38) Izuhara, D.; Swager, T. M. *J. Am. Chem. Soc.* **2009**, *131*, 17724–17725.
- (39) See, K. C.; Feser, J. P.; Chen, C. E.; Majumdar, A.; Urban, J. J.; Segalman, R. A. *Nano Lett.* **2010**, *10*, 4664–4667.

AM100654P